



Surface Enhanced Raman Spectra and Theoretical Study of an Organophosphate Malathion

T. ASENATH BENITTA^{1*}, SUDHIR KAPOOR², SHEELA CHRISTY R¹,
ISAC SOBANA RAJ C¹ and THAMPITHANKA KUMARAN J³

¹Nesamony Memorial Christian College, Marthandam, Tamilnadu, India.

²Radiation & Photochemistry Division, Bhabha Atomic Research Centre, Mumbai 400085, India.

³Malankara Catholic College, Mariagiri, Kaliyakavilai, Pin - 629153, Tamilnadu, India.

*Corresponding author E-mail: tasenathbenitta@yahoo.co.in

<http://dx.doi.org/10.13005/ojc/330223>

(Received: January 27, 2017; Accepted: March 25, 2017)

ABSTRACT

Surface Enhanced Raman Scattering (SERS) is an established technique for the rapid and sensitive analysis of chemicals, pesticides and pharmaceuticals. The aim of this work is to develop sensitive and cost effective SERS substrates for pesticide detection using modified mirror reaction and physical deposition method. The prepared substrates were examined using Field Emission Scanning Electron Microscope (FESEM). The prepared slides were then used to detect an organophosphate pesticide, Malathion. The available simple geometry of Malathion was optimized using 6-311++G(d,p) basis set of Gaussian 09 software. The experimental Raman spectra, Surface Enhanced Raman spectra and theoretically computed wavenumbers are compared and the results are presented briefly.

Keywords: Malathion, FESEM, modified mirror reaction, nanocluster deposition.

INTRODUCTION

Wrong agricultural habits have caused an adverse effect to human health and environment because toxic and biologically harmful substances are used as insecticides¹. Insecticides used to increase the yield in agriculture are sometimes pollutants. Organophosphate pesticides are compounds of toxic agents used as insecticides in several Asian countries. They cause harmful effects to human life, such as irritation to eyes, sensory

disturbances and respiratory depression. Due to the environmental concerns related with the excess accumulation of pesticides in food products and their toxic effects, a focus on insecticide detection at trace concentration is essential. A number of faster and sensitive detection systems for the identification and analysis of insecticides is available in literature²⁻⁴. The earlier methods for insecticide detection based on gas chromatography, are time consuming, complex and labor intensive with a possibility of incomplete assessment due to limited database

mapping. They also require expensive and bulky equipment, and hence are not portable. All these are overcome by SERS which has several advantages over other spectroscopic techniques due to its accuracy, portability and sensitivity.

Surface Enhanced Raman Spectroscopy is proven to be a powerful tool for chemical and biomolecule detection. More interest in using SERS technique is shown in the analysis of food contaminants, chemical additives and pesticide residues. Compared to the conventional chromatographic procedures, simple sample preparation and detailed analysis can be achieved by SERS. With the advancements in nanotechnology, more sensitive and reliable SERS substrates are fabricated. Noble metal nanostructures or nanoparticles provide enormous enhancement to the Raman scattering process. A large magnitude of enhancement is attained which places the sensitivity of SERS to a higher level, compared to the sensitivity of fluorescence based detection.

A compact Raman spectroscopy system, using silver nanorod film fabricated by magnetron sputtering is already in use for field portable pesticide detection⁵. The obtained results specify a sensitive detection for the trace organic analysis of toxic chemical agents. It has been reported that nanoparticles of gold and silver in solution state, are effective systems for the removal of two common pesticides (Chlorpyrifos and Malathion) from water⁶. The time dependent removal of these pesticides from water has been monitored by UV-Visible spectroscopy and the adsorption of pesticides on nanoparticles have been confirmed with infrared spectroscopy. This method provides a new technology for drinking water purification, particularly by using silver nanoparticles.

A new format of apta-sensing based on polymer gold nanoparticle for SERS detection of Malathion has already been performed⁷. A rapid, simple and eco-friendly method using micro Raman spectroscopy for the determination of pesticide residues of Dimethoate, Chlorpyrifos and Malathion on the surface of fruits has been reported⁸. Based on the results, it has been concluded that micro Raman spectroscopy can be utilized for the determination of pesticide residues on the surface of fruits.

This paper deals with the development and applications of SERS in the chemical analysis of food, mainly focusing on pesticides. The main objective in this work is to fabricate highly sensitive, reliable and cost effective SERS substrates using modified mirror reaction (MMR) and physical deposition by cluster deposition system (AgNC). The prepared substrates examined using FESEM were used to detect various concentrations of Malathion. Geometry optimization of Malathion was performed using 6-311++G(d,p) basis set of Gaussian 09 software⁹ and the theoretical vibrational frequencies were simulated from the same software. The experimental Raman spectra, SERS and theoretically simulated Raman spectra are compared.

Experimental details

In the present study, the substrates were prepared chemically by modified mirror reaction. In brief, a fine brown precipitate of Ag_2O was produced by adding 20 μL of 3.2 wt. % KOH solution in 18 mL of a 2 wt. % AgNO_3 solution. The precipitate was dissolved by adding ammonium hydroxide (29.5%) drop by drop. Then 6 wt. % AgNO_3 solution was added and the solution turned yellow. The solution became colourless on adding a drop of 6 wt. % ammonium hydroxide solution. Then 3 mL methanol, 10 μL 10 wt. % $\text{Na}_3\text{P}_5\text{O}_{10}$, and 40 μL of 5 wt. % Na_2HPO_4 was added consecutively to form a yellow colloid. Finally, 6 mL 35 wt. % glucose was added, which yielded a colloidal solution. Glucose acts as a fixing agent. Nano particles form even in the absence of glucose.

The glass slides were cut in to the dimension of 7.5 cm x 2.5 cm and was cleaned with Piranha solution for few minutes or until the visible reaction of organic material with the solution stops. The Piranha solution is a mixture of three parts of concentrated H_2SO_4 and one part of H_2O_2 (29.5%) [3:1]. The glass slides were then rinsed with Milli Q water (resistivity 18.2 $\text{M}\Omega\text{cm}$). To clean the glass slides further, it was sonicated in propanol, acetone and Milli Q water and then dried under nitrogen gas. The cleaned glass slides were immersed in the colloidal suspension for 24 hours at room temperature to form Ag nano-film on them. The substrates were taken out and rinsed with copious amount of Milli Q water and dried under nitrogen gas. These substrates were then heated for 3 hours at 200°C in the vacuum oven kept inside

the anhydrous conditions of an argon glove box by maintaining O₂ and H₂O level less than 0.1 ppm to remove oxidation product, if any.

Substrates of silver nano particles were also made by physical deposition of silver nano particles on glass slides. The Nanodep60 nanocluster deposition system from Oxford Applied Research UK produces nano particles of high purity and with practically no chemical contamination. This deposition system is based on the principle of inert gas phase condensation. In this deposition method, a silver plate is sputtered using a DC magnetron source and the sputtered silver atoms move in to the aggregation zone under an inert gas flow. The super saturated metal atoms while flowing through the inert carrier gas, nucleates and forms clusters of nanometer scale. The sputtering based cluster source can produce a large range of mean cluster sizes from 200 to 15000 atoms per cluster, and a wide variety of elements and alloys can be used as source materials.

The nanoclusters formed in the aggregation chamber are made to flow through an aperture into the deposition chamber where the glass slides are kept for deposition. The deposition chamber is maintained at a slightly low pressure than the aggregation chamber by differential pumping. The distance between the substrate and aperture was approximately 55 cm. The base pressure in the system before the start of deposition was 4×10^{-7} milli bar and a working pressure of 5×10^{-5} milli bar was obtained during the aggregation gas (Ultra high pure Argon of 99.999% purity) flow where the flow rate was maintained at 100 sccm (standard

cubic centimeter per minute). The current in the DC magnetron was held constant at 0.2 A and the power level was about 70 Watts

RESULTS AND DISCUSSIONS

Surface Characterization

The morphology of Ag nanoparticles prepared by modified mirror method was examined using FESEM. It can be seen from the FESEM image shown in Fig. 1 that Ag nanoparticles of the order of 20 nm was obtained and distributed uniformly on the slides surface. The efficiency of the substrate was then tested using Crystal Violet (CV) solution. For this the CV was diluted in milli Q water by sequential dilution method and few drops were put over the prepared substrate using a micro pipette. SERS was recorded for the substrate with CV and the observed peaks were more or less similar to that reported in literature ¹⁰. An attempt was made to deposit silver nanoparticles by physical deposition using cluster deposition system. It was made possible to get

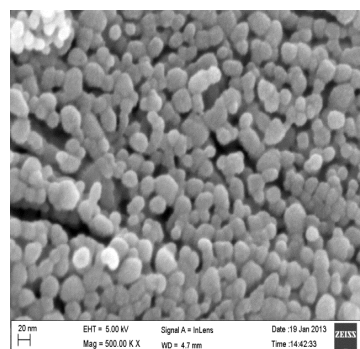


Fig.1: FESEM image of the substrate prepared by Modified mirror reaction.

Table 1: Vibrational frequencies and assignments of Malathion along with potential energy distribution (PED) .

Simulated wavenumber (cm ⁻¹)	SERS wave number(cm ⁻¹)	Expt. Raman [8] (cm ⁻¹)	Atoms	Assignments
1783	1696	1733	O15=C9	C=O stretch (85%)
1387	1349	-	H2-C1-H4	H-C-H bend (14%)
1333	1345	-	H6-C5-C1	H-C-C bend (55%)
1329	1267	-	H33-C32-C35	H-C-C bend (64%)
1022	-	1022	C1-C5	C-C stretch (76%)
644	-	652	P17=S18	P=S stretch (77%)

somewhat clean Ag particles over the substrate using this method. The FESEM of this substrate is shown in Fig. 2. It is seen from the FESEM image that the silver nano particles were of the order of 40 nm.

Vibrational Analysis

The vibrational frequencies were calculated using the triple split valence basis set 6-311++G(d,p) which includes diffuse and polarization functions. The vibrational bands assignments corresponding to the vibrational frequencies were elucidated by means of potential energy distributions (PEDs) using VEDA 4 program¹¹. As SERS spectra is recorded in the range 400-2000 cm^{-1} only a partial vibrational analysis is presented. Optimized geometry of Malathion is shown in Fig 3. The vibrational frequencies, their assignments and the atoms involved are presented in Table 1.

The P=S bond shows a strong stretch band at 652 cm^{-1} in the reported Raman spectrum of Malathion⁸. A simulated wavenumber at 644 cm^{-1} supports this. The bands located at 1022, and 1733

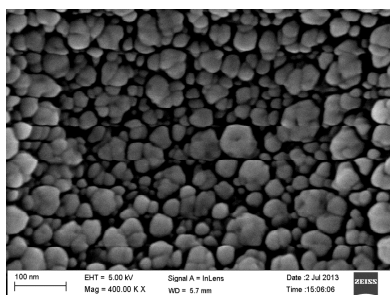
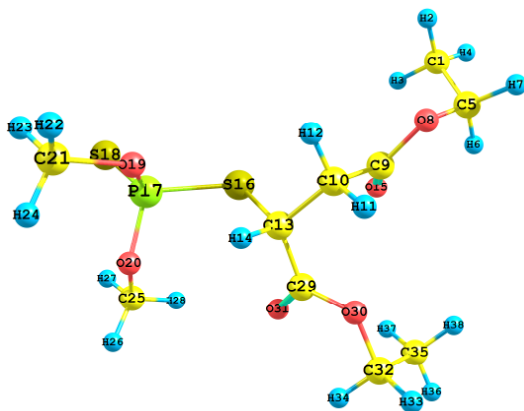


Fig. 2: FESEM picture of the substrate prepared by nano cluster deposition



wavenumber at 644 cm^{-1} having a PED of about 77 % is assigned to P=S stretching. The same effect is also seen in the medium weak band at 1022 cm^{-1} due to C-C stretching present in the Raman spectrum but absent in SERS. This is seen in the simulated wavenumber at 1022 cm^{-1} and has a PED of 76 %. A simulated wavenumber of 1329 cm^{-1} is assigned to H-C-C bending of the methyl group (numbered as 35, 36, 37, 38) and methylene group (numbered as 32, 33, 34). It has a PED of 64% .

This is obtained as a weak SERS signal at 1267 cm^{-1} corresponding to the H-C-C bending vibration. All the above results clearly shows that all these vibrations corresponding to the first 8 atoms of Malathion along with C=O stretching and atoms of the methyl and methylene group lie close to the Ag substrate and sticks to it. By fixing two atoms on

the XY plane, the optimized geometry of Malathion was rotated with the help of a C++ program such that two atoms corresponding to strong SERS signals had minimum negative value. It was found that the atoms H4, C9 were placed on the XY plane and sticks to the silver substrate.

The first element to be noted in a new SERS active substrate is sensitivity. From the SERS spectra it was found that the substrate exhibits good enhancement ability, and is highly sensitive. Another prime factor for SERS detection is reproducibility of the substrate. The SERS spectra was recorded for various concentration of Malathion by taking an average of ten randomly selected locations. This average is reproducible. Further the strong SERS signals suggest the presence of hot spots over the substrate, resulting in high reproducibility. It is

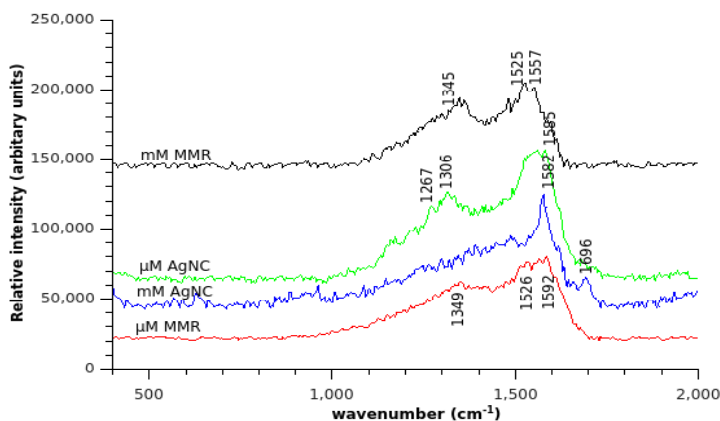


Fig. 4: Comparative figures of SERS spectra at different concentrations of Malathion.

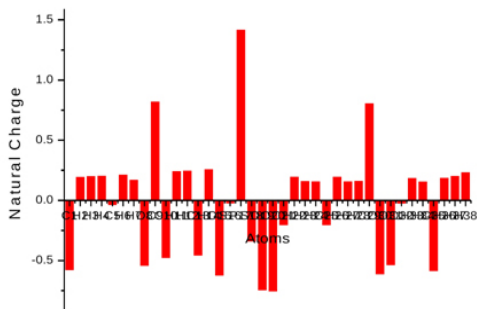


Fig. 5: Natural charges for various atoms of Malathion obtained from Gaussian software.

Table 2: Second Order Perturbation Theory Analysis of Fock Matrix in NBO Basis

Donor NBO (i)	E.D (e)	Acceptor NBO (j)	E.D (e)	$E^{(2)}$ kJ mol ⁻¹
n(1)O ₈	1.96220	$\sigma^*(C_9-O_{15})$	0.02337	34.392
	-0.57498		0.60045	
n(1)O ₂₀	1.94464	$\sigma^*(P_{17}-S_{18})$	0.08050	17.112
	-0.58311		0.16051	
n(1)O ₂₀	1.94464	$\sigma^*(C_{25}-H_{26})$	0.01022	10.543
	-0.58311		0.39219	
n(1)O ₃₀	1.96206	$\sigma^*(C_{29}-O_{31})$	0.02249	32.969
	-0.57813		0.60576	

pertinent to mention that the prepared substrates has a detection limit of 0.002 ppm. The sensitivity obtained from colloidal gold nanoparticles based on Lee-Meisel method for the detection of Malathion was 0.123 ppm¹³.

NBO Calculations

The Natural Bond Orbital (NBO) calculation were performed using NBO 3.1 program¹⁴ available in the Gaussian'09 software package, to understand various second-order interactions between the filled orbitals of one subsystem and vacant orbitals of another subsystem.

Natural Charge Analysis

The natural charge analysis on the electronic structure of Malathion describes the distribution of charges of the atoms in the molecule. Distribution of positive and negative charges are important in increasing or decreasing the bond length between atoms. In this molecule oxygen and carbon atoms exhibits negative charges, and are donors. Hydrogen atoms have positive charge, and they are acceptors. The various positive and negative charges obtained from natural charge analysis can be plotted in a graph

and is shown in Fig 5. The highest positive charge is obtained as 1.596 e for P17

Natural Bond Orbital Analysis

NBO analysis provides a basis for intermolecular charge transfer or conjugative interactions in molecular systems. For each donor NBO (i) and acceptor NBO (j), the stabilization energy $E^{(2)}$ associated with electron delocalization between donor and acceptor is estimated as

$$E^{(2)} = \Delta E_{ij} = q_i \frac{F(ij)^2}{\epsilon_j - \epsilon_i} \quad \dots(1)$$

where q_i is the i^{th} donor orbital occupancy, ϵ_i and ϵ_j are diagonal elements and $F^{(ij)}$ is the off diagonal NBO Fock matrix element. Some electron donor, acceptor orbitals and the interacting stabilization energy resulting from second order micro disturbance theory have been reported^{15, 16}.

In NBO analysis large $E^{(2)}$ value shows strong intramolecular hyperconjugative interactions between the atoms of the molecule. The second order perturbation theory analysis of Fock matrix in

Table 3: Zero point vibrational energy, HOMO-LUMO energy gap, Chemical potential, Hardness and Electrophilicity index of Malathion

Zero point vibrational energy (kJ/mol)	Dipole moment (Debye)	SCF energy (a.u)	HOMO-LUMO energy gap (eV)	Chemical potential (μ) (eV)	Hardness (η) (eV)	Electrophilicity index (ω) (eV)
784.27	5.759	-1981.996	3.510	5.2414	1.7632	7.790

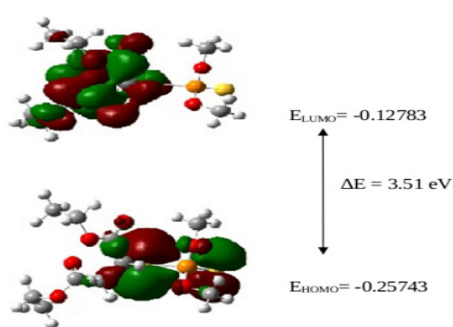


Fig. 6: The molecular orbitals and energies of HOMO and LUMO for Malathion

NBO basis for Malathion is shown in Table 2. The lone pair interactions between $n_1(O_8) \rightarrow \sigma^*(C_9-O_{15})$, $n_1(O_{30}) \rightarrow \sigma^*(C_{29}-O_{31})$, $n_1(O_{20}) \rightarrow \sigma^*(P_{17}-S_{18})$ obtained as 34.39, 32.97 and 17.11 kJ/mol, respectively serves as an evidence for charge transfer interactions. The lone pair $n_1(O_{20})$ interaction with the anti bonding orbital ($C_{25}-H_{26}$) reveals the presence of C-H...O intramolecular hydrogen bonding.

HOMO-LUMO Analysis

Frontier molecular orbitals (lowest unoccupied molecular orbital (LUMO) and highest occupied molecular orbital (HOMO)) play an important role in the electric and optical properties

of compounds ¹⁷. The frontier orbital gap helps to understand the chemical reactivity and kinetic stability of the molecule ¹⁸. The molecular orbitals and energies for HOMO and LUMO is shown in Fig 6. The HOMO presents a charge density localised around the phosphorothyl and carbonyl groups. LUMO is characterised by a charge distribution on ethyl, methyl and carbonyl groups present in the compound.

The energy difference between the highest occupied molecular orbital and the lowest unoccupied molecular orbital in Malathion was found to be 3.51 eV. Low HOMO-LUMO energy gap value predicts the eventual charge transfer interactions taking place within the molecule and suggests that the molecule is bioactive.

The values of hardness and chemical potential of Malathion, can be evaluated from the HOMO and LUMO orbital energies using the following approximate expressions

$$\mu = -\frac{E_{HOMO} + E_{LUMO}}{2} \quad \dots(2)$$

$$\eta = -\frac{E_{LUMO} - E_{HOMO}}{2} \quad \dots(3)$$

where μ is the chemical potential, and η is the hardness ^{19,20}. To evaluate the electrophilicity of Malathion, the electrophilicity index, ω can be measured using the expression ²¹.

$$\omega = \frac{\mu^2}{2\eta} \quad \dots(4)$$

The theoretically calculated HOMO-LUMO energy gap, dipole moment, chemical potential and electrophilicity index are listed in Table 3

CONCLUSION

Organophosphate pesticide Malathion was detected and analysed using the SERS substrates prepared by modified mirror reaction and physical deposition method. A much better basis set 6-311++G(d,p) including diffuse and polarization functions was used for Malathion using Gaussian 09 software. From the SERS spectra obtained for this pesticide, the prepared substrate was suitable as a highly sensitive SERS substrate and a detection limit of 0.002 ppm was obtained. Substrates prepared by modified mirror reaction and physical deposition are highly sensitive, reproducible and cost effective. The obtained results indicate that this method can be used for sensitive detection and analysis of other toxic chemical agents and pesticides.

ACKNOWLEDGEMENT

The authors would like to acknowledge the financial support of DAE-BRNS for the project no 2012/34/1/BRNS/No.122 dated 12 April 2012.

REFERENCES

1. Database on Pesticides consumption, Food and agriculture organization of the United nations, statistical analysis service, Rome, Italy **1950**.
2. Lehotay, S.J.; Son, K.A.; Kwon H.; Koesukwiwat U.; Fu W.; Mastovska K., *Journal of Chromatography A*, **2010**, *1217* (16), 2548–2560
3. Molto, J.C.; Pico Y.; Font G.; Manes D., *Journal of Chromatography A*, **1991**, *555*, 137-145.
4. Tonogai Y.; Tsumura Y.; Nakamura Y.; Ito Y.; Watanabe Y.; Shiomi Y., *Journal of Chromatography A*, **1993**, *639*, 352-358
5. Article in proceedings of spie - the International Society for Optical Engineering February **2011**. <http://www.researchgate.net/publication/260451739>
6. Sreekumaran Nair A.; Pradeep T. *Journal of Nanoscience and Nanotechnology*, **2007**, *7*, 1-7.
7. Francisco Barahona; Cameron L. Bardliving; Adrienne Phifer; John G. Bruno and Carl A. Batt, *Industrial Biotechnology*, **2013**, *9*(1), 42-50.
8. Yande Liu; Tao Liu. *Computer and Computing*

- Technologies in Agriculture IV*, Volume 347 of the series IFIP Advances in Information and Communication Technology **2010**, 427-434.
9. Frisch M.J.; Trucks G.W.; Schlegel H.B.; Scuseria G.E.; Robb M.A.; Cheesman J.R.; Zakrzewski V.G.; Montgomery, Jr. J.A.; Stratmann R.E.; Burant J.C.; Dapprich S.; Millam J.M.; Daniels A.D.; Kudin K.N.; Strain M.C.; Farkas O.; Tomasi J.; Barone V.; Cossi M.; Cammi R.; Mennucci B.; Pomelli C.; Adamo C.; Clifford S.; Ochterski, J.; Petersson G.A.; Ayala P.Y.; Cui Q.; Morokuma K.; Rega N.; Salvador P.; Dannenberg J.J.; Malich D.K.; Rabuck A.D.; Raghavachari K.; Foresman J.B.; Cioslowski J.; Ortiz J. V.; Baboul A.G.; Stetanov B.B.; Liu G.; Liashenko A.; Piskorz P.; Komaromi I.; Gomperts R.; Martin R.L.; Fox D.J.; Keith T.; Al-Laham M.A.; Peng C.Y.; Nanayakkara A.; Challacombe M.; Gill P.M.W.; Johnson B.; Chen W.; Wong M.W.; Andres J.L.; Gonzalez C.; Head-Gordon M.; Replogle E.S.; Pople J.A. *GAUSSIAN 98*, Revision A 11.4, Gaussian, Inc, Pittsburgh PA, **2009**.
 10. Botta R.; Upender G.; Sathyavathi R.; Narayana Rao D.; Bansal C. *Materials Chemistry and Physics*, **2013**, *137*, 699-703.
 11. Jamroz M. H. *Vibrational Energy Distribution Analysis VEDA 4*, Warsaw, **2004**.
 12. Quintas G.; Garrigues S.; M. de la Guardia, *Talanta*, **2004**, *63* 345-350.
 13. Albuquerque C.D.L.; Poppi R.J. *Analytica Chimica Acta* **2015**, *879*, 24-33.
 14. Glendening E.D.; Reed A.E.; Carpenter J. E.; Weinhold F. *NBO Version 3.1*, University of Wisconsin, Madison, **1998**.
 15. James C.; Amal Raj A.; Reghunathan R.; Hubert Joe I.; Jeya Kumar V. S. *Journal of Raman Spectroscopy*, **2006**, *37*, 1381-1392.
 16. Liu J.N.; Chen Z.R.; Yuan S.F. *Journal of Zhejiang University Science B*, **2005**, *6*, 584-589.
 17. Fleming I. *Frontier Orbitals and Organic Chemical Reactions*, John Wiley & Sons, London, **1976**.
 18. Kosar B.; Albayrak C. *Spectrochimica Acta Part A*, **2011**, *78*, 160-167.
 19. Pearson R.G.; *Chemical Hardness*, Wiley-VCH, Oxford, **1997**.
 20. Parr R.G.; Yang W. *Density Functional Theory of Atoms and Molecules*, Oxford University Press, New York, **1989**.
 21. Parr R.G.; Szentpaly L.v.; Liu S. *Journal of the American Chemical Society*, **1999**, *121*(9) 1922-1924.